Journal Pre-proof

https://doi.org/10.1016/j.compositesb.2020.108211

PII: S1359-8368(20)33261-3

DOI: https://doi.org/10.1016/j.compositesb.2020.108211

Reference: JCOMB 108211

To appear in: *Composites Part B*

Received Date: 19 April 2020

Revised Date: 1 June 2020

Accepted Date: 5 June 2020

Please cite this article as: Quinsaat JEQ, de Wild T, Nüesch FA, Damjanovic D, Krämer R, Schürch G, Häfliger D, Clemens F, Sebastian T, Dascalu M, Opris DM, Stretchable piezoelectric elastic composites for sensors and energy generators, *Composites Part B*, https://doi.org/10.1016/j.compositesb.2020.108211.

Re. Manuscript JCOMB_2020_2463

Dear Editor, dear Professor Thomsen,

Thank you very much for your mail of May 10, 2020 indicating that our submission Composites Part B: Engineering entitled “Stretchable piezoelectric elastic composites for sensors and energy generators" might be accepted after an appropriate consideration of the reviewers’ remarks.

Please find the CRediT authorship contribution statement outlining the contributions of each author of this manuscript as it follows:

CRediT authorship contribution statement

Jose Enrico Q. Quinsaat: Investigation, Methodology, Formal analysis, Writing-original draft. **Tym de Wild:** Formal analysis, Writing-review & editing. **Frank A. Nüesch:** Funding acquisition, Supervision, Writing-review and editing. **Dragan Damjanovic:** Writing-review & editing. **Ronny Krämer:** Investigation, Formal analysis. **Georg Schürch:** Investigation, Formal analysis**. Daniel Häfliger:** Funding acquisition, Supervision. **Frank Clemens:** Writing-review & editing. **Tutu Sebastian:** Writing-review & editing. **Mihaela Dascalu:** Investigation, Formal analysis, Writing-review & editing. **Dorina M. Opris:** Funding acquisition, Supervision, Investigation, Formal analysis, Writing-original draft.

Kind regards,

Jose Enrico Q. Quinsaat and Dorina M. Opris

Stretchable piezoelectric elastic composites for sensors and energy generators

Jose Enrico Q. Quinsaat,[1]* Tym de Wild,[1,2] Frank A. Nüesch,[1,2] Dragan Damjanovic,[3] Ronny Krämer,[4] Georg Schürch,[4] Daniel Häfliger,[4] Frank Clemens,[5] Tutu Sebastian,[5] Mihaela Dascalu,[1] Dorina M. Opris[1]*

[1]Swiss Federal Laboratories for Materials Science and Technology Empa, Laboratory for Functional Polymers, Ueberlandstr. 129, CH-8600, Dübendorf, Switzerland

[2]Ecole Polytechnique Fédérale de Lausanne (EPFL), Institut des Matériaux, Station 12, CH 1015, Lausanne, Switzerland

[3]Ecole Polytechnique Fédérale de Lausanne (EPFL), Group for Feroelectrics and Functional Oxides, Station 12, CH 1015, Lausanne, Switzerland

[4]Sateco AG, Tumigerstr. 111, CH-8606, Naenikon-Uster, Switzerland

[5]Swiss Federal Laboratories for Materials Science and Technology Empa, Laboratory for High Performance Ceramics, Ueberlandstr. 129, CH-8600, Dübendorf, Switzerland

E-mail: jose.quinsaat@gmx.ch

E-mail: dorina.opris@empa.ch

Keywords: piezoelectric composites, piezoelectric elastomers, sensors, energy generators, silicone composites

Abstract

The search for a piezoelectric elastomer that generates an electrical signal when pressed and stretched has increased significantly in the last decade as they hold great promise in harvesting energy from human motion and monitoring human activities. Here, the excellent elasticity of polydimethylsiloxane-based elastomers and the piezoelectric properties of lead zirconate titanate (PZT) were combined and, using a thermally activated poling process, elastic piezoelectric composites were obtained. For this, two polydimethylsiloxane (PDMS) matrices with a molar mass of 139 kDa and 692 kDa and PZT fillers with particle sizes of 2 and 20 μm were used. For the same poling conditions, an increase in the piezoelectric response with increasing amount of filler, filler size and molar mass of the polymer matrix was observed. Overall, d^*_{33} and d^*_{31} values of 2.7−40 $pC \cdot N^{-1}$ and 16−48 $pC \cdot N^{-1}$ were achieved in this work with filler contents ranging from 37−72 vol.%. A composite material with a PZT filler content of 38 vol.% (20 μm particle size) in a commercially available PDMS with a M_w =139 $kg \cdot mol^{-1}$ exhibited high flexibility, good elasticity with long-term mechanical stretchability and high lon-

gitudinal and transverse piezoelectric coefficients of 3.6 $pC \cdot N^{-1}$ and 30 $pC \cdot N^{-1}$, respectively. The higher transverse piezoelectric constant d^*_{31} can be explained by an additional capacitor effect of the composite film structure. These properties are interesting features for energy conversion from human motion, monitoring human activities, and stretchable electronics. The functionality of the newly developed material is demonstrated in a pressed sensor.

Introduction

Piezoelectric materials have the characteristic of generating an electrical signal by an induced mechanical stress and vice versa, described by the converse and direct piezoelectric effect. They have been used in a wide range of applications such as ultrasound tranducers, sensors, actuators and energy harvesters.[1,2] Piezoelectricity can be found in both organic and inorganic materials, whereas ferroelectric ceramics exhibit by far the highest response. For instance, perovskite ceramics such as barium titanate (BTO)[3,4] or lead zirconate titanate (PZT)[5,6] have a high d^*_{33} piezoelectric coefficient, high temperature stability and a high dielectric constant, which render them attractive for energy conversion materials. Below their Curie temperature T_c, BTO (T_c = 130 °C) and PZT ($T_c \geq$ 360 °C) feature a tetragonal or rhombohedral structure with a non-symmetric distribution of the central atom. To obtain a piezoelectric effect in a ferroelectric ceramic with randomly distributed grains, the polarization within different grains must be oriented as much as possible in the same direction. This can be achieved by subjecting the ferroelectric materials to a strong electric field *via* a so-called poling process, where it is assumed that the microscopic polar domains within the crystal structure are reoriented and a permanent polarization is introduced in the macroscopic sample, leading to a high piezoelectric response of the poled material. However, ceramics are brittle and therefore their application in flexible electronics is limited. Although more flexible alternatives such as poled polylactic acid [7], polyvinylidene difluoride [8,9] or disperse red 1-*co*-polymethylmetacrylate composite in polydimethylsiloxane (PDMS) [10,11] exist, their piezoelectric response is relatively weak compared to ferroelectric ceramics. To increase the piezoelectric properties of polymeric materials, often a ferroelectric powder is mixed inside a polymeric matrix such as lead zirconium titanate (PZT), barium titanate or bismuth ferrite.[2,12–14] Sebastian *et al*. demonstrated that even flexible polymer-based composite fibers with a 60 vol.% of ferroelectric fillers could be polarized by applying an electrical field up to 4 $kV \cdot mm^{-1}$.[15] In order to achieve elasticity, ceramic particles can be dispersed in an elastic matrix such as PDMS, thus leading to mechanically stable materials. Such composites can undergo high deformation strain, which is an interesting feature for energy conversion from human

motion, monitoring human activities and stretchable electronics.[16–18] In recent years, implantable piezoelectric biomedical devices which were powered by motions in the human body such as breath and heartbeat into electrical energy were developed which could pave the way for sustainable future health care technologies.[19–21]

In this work, PZT particles of two different sizes are dispersed in two different high molecular weight PDMS matrices and the composites are poled in an electric field to enhance their respective piezoelectric properties, e.g., the d^*_{33} and d^*_{31} coefficients. These two coefficients represent the ability of a material to convert a pressure applied in poling direction (d^*_{33}) or a tensile stress perpendicular to the poling direction (d^*_{31}) into electric charge, which is exploited in sensor applications. We achieved highly stretchable materials with a filler content of 37−66 vol.%, which show a d^*_{33} value of 2.7−40 pC·N^{-1} and d^*_{31} value of 16−48 pC·N^{-1} and therefore exhibit attractive properties for sensors and energy harvesters. While the d^*_{33} values of PZT/PDMS composites have been extensively reported previously and used as a basis for sensor development, the d^*_{31} measurements of the corresponding composites was hardly studied, hence the potential of exploiting this feature of PZT/PDMS for energy harvesting was an integral part of this investigation. [2,12,22–26] Additionally, stability measurements were conducted to check the performance of selected composites after subjecting them to different environmental treatmetns such as humidity and temperature. Furthermore, we demonstrated that the longitudinal piezoelectric effect of the prepared composite materials can be utilized to construct a working prototype sensor.

Experimental Part

Materials

Formulation components

PZT powders (T & P5s, grain size 2 and 20 µm according to the distributor) were purchased from T & Partners, Praha (PZT Division). The powder has a density of 7.6 g/cm^3, a dielectric constant ε' of 2'100 and piezoelectric constants d^*_{33} of 450 pC·N^{-1}, respectively. Sodium carbonate (Na_2CO_3) was purchased from Sigma Aldrich. Linear silanol end-functionalized polydimethylsiloxane (M_w = 139 kg·mol^{-1}) denoted as PDMS 139k, octamethyltetracyclosiloxane (D4) and (25–35% methylhydrosiloxane)–dimethylpolysiloxane copolymer were obtained from ABCR, dibutyltindilaurate (DBTDL) and hexamethyldisilazane (HMDS, >98 %) both from Alfa Aesar, and toluene, chloroform, sulphuric acid (H_2SO_4) from VWR, linear silanol end-functionalized polydimethylsiloxane (M_w = 692 kg·mol^{-1}) denoted as PDMS 692k was

prepared according to the literature through the acid-catalyzed ring-opening polymerization of D4.[27] Graphite nanoplatelets (GNP, xGNP-M-25, 6−8 nm × 25 µm sheets) were purchased from XG Sciences Inc., USA and carbon black (Ketjenblack EC-600 JD, primary particle diameter 34 nm) from Akzonobel. The electrode material used GNPs/CB (300/150 30 wt.%) in PDMS, which was prepared according to the literature.[28]

Hydrophobization of PZT

To a dispersion of PZT powder (37 g) in toluene (640 mL) prepared *via* tip sonication (~5 min), HMDS (57 mL) was added under argon atmosphere at room temperature and stirred at 40 °C overnight. Then, the powder was recovered through centrifugation and decantation of the solvent. After a washing cycle consisting of redispersing the precipitate in toluene, the suspension was centrifuged, and the liquid was decanted again. The washing cycle was repeated thrice. The trimethylsilyl surface-modified PZT particles were kept wet for the preparation of composites.

Synthesis of high molecular weight linear silanol end-functionalized PDMS

D_4 was introduced in a reaction vessel equipped with mechanical stirrer and cooling mantle. Concentrated H_2SO_4 was added as a catalyst and the reaction mixture was vigorously stirred for 60 min at 25 °C, after that distilled water (2 mL) was added and the stirring was continued for another 30 min. The mixture was stored as such for 18.5 h. The polymer was dissolved in a large amount of $CHCl_3$ (~ 2.5L), followed by repeatedly washed with an aqueous solution 5% Na_2CO_3 and warm water

In order to reach a neutral pH, followed by the removal of $CHCl_3$ at the rotary evaporator. The polymer was further dried in a vacuum oven at 150 °C for several hours in order to remove residual cycles which were present as side products of the reaction.

The molecular weight of the polymer (M_w = 692 kg·mol^{-1}, PDI = 5.01) was determined from gel permeation chromatography (GPC) measurements (Supporting Information SI 1).

PDMS composites

The trimethylsilyl surface-modified PZT powder (7−24 g) dispersed in toluene (~10 mL) by tip sonication for 2 minutes was mixed with PDMS 139k or 692k (1.5 g) and (25–35% methylhydrosiloxane)–dimethylpolysiloxane (150 µL) in the three-roll-mill (Exakt, type 80 S) for 10 min. Thereafter, the composite was redispersed in toluene, stirred at room temperature for aproximately 2 hours, treated with a 50% solution of DBTDL in toluene (112 µL). The mixture was then bath sonicated for 5 minutes, and then casted onto a fluorinated polymer substrate using a doctor blade. The composites were let to stand at room temperature overnight and then heated in *vacuo* for 7 hours at 80 °C before further investigations. The composites had a film thickness of 170−250 µm (PDMS 139k) and 120−150 µm (PDMS 692k).

Characterization Methods

SEM images were obtained with a Nova NanoSEM 230 FEI and the investigated samples were sputtered with Au prior to the measurement. TGA was conducted with a Perkin Elmer TGA7 at a heating rate of 20 °C min^{-1} under a He gas flow. Impedance spectroscopy measurements were performed at room temperature with a Novocontrol high impedance Alpha Analyzer using a Hewlett Packard 16451B dielectric test fixture equipped with round electrodes on circular composite samples with round sputtered gold electrodes (20 mm diameter, 20 nm thickness) on both sides. The measurements were performed in a frequency range between 0.1–10^6 Hz. The amplitude of the probing ac electric signal applied to the samples was 1V, and the permittivity ε' was determined from the capacitance: $C=\varepsilon'\varepsilon_0 A/d$, where A is the electrode area, d is the thickness of the film and ε_0 is the vacuum permittivity. The permittivity values were averaged from the deviation in the film thickness of the corresponding film sample. Tensile tests were performed using a Zwick Z010 tensile test machine with a crosshead speed of 50 mm·min^{-1}. Tensile test samples, with a gauge width of 2 mm and a gauge length of 18 mm, were prepared by die-cutting. The strain was determined using a longitudinal strain extensometer. Stress versus strain curves were obtained by averaging measurements of 3 to 5 samples for each material. The Young's modulus was determined from the slope of the stress–strain curves at ≤ 10 % strain. Dynamic mechanical analysis (DMA) was carried out on an RSA 3 DMA from TA Instruments. Strips of 10 mm × 20 mm from selected samples

were measured under a dynamic load of 2 g, at 2% strain in the frequency range of 0.1–10 Hz at 25 °C. The mechanical loss factor *tan(δ)* is given as the fraction of imaginary and real storage modulus at 2% strain.

Gel permeation chromatography (GPC) measurements were done with an Agilent 1100/PSS WinGPC 8.1 system in THF (flowrate: 1 mL/min) calibrated with PDMS standards (Polymer Standards Service). The dielectric breakdown was determined using flat rigid metal electrodes with an area of 0.25 mm^2 embedded in an epoxy resin, which hindered electromechanical actuation of the dielectric films. Ten measurements were conducted for each sample.

Poling

The composite was sandwiched between two 15 mm (diameter) flexible electrodes, consisting of GNPs/CB (300/150 30 wt.%) in PDMS, and two 15 mm (diameter) round aluminum electrodes. The metal electrodes were then connected to a voltage source and to the ground. Most composites were poled in an electric field of 3−18 $V \cdot \mu m^{-1}$ at 150 °C for 40 min and afterwards cooled to room temperature at a rate of 4 °C min^{-1} with the field still switched on. This precaution was used to avoid the relaxation of the domains back to their random orientation. The field was maintained by a Stanford Research Systems PS350 high voltage source. Temperature control was ensured by a Lauda RC6 CP thermostatic oil bath connected to a closed glass container that housed the composite.

The d^*_{33} piezoelectric coefficient was measured by applying a constant force (0.6 N) on the poled part of the composite, which is covered by the electrode material, that led to a voltage output. The measuring device was calibrated with a reference ceramic sample with a d^*_{33} of 17.5 $pC \cdot N^{-1}$ in order to calculate the resulting d^*_{33} coefficient. The samples measured had two conductive electrodes on them, which were applied according to a previous procedure.[28]

For the d^*_{31} measurements, a Zwick Z010 tensile testing machine was used to apply strain and measure the force acting on the rectangular films with dimensions of 3.5 cm × 2.5 cm (length × width). The metallic clamps of the tensile testing machine were covered with a layer of adhesive tape to insulate them from the sample. A strip of adhesive copper tape was attached to both the upper and lower clamps to make an electrical connection between the sample and the voltage readout via a current preamplifier. Both sides of the poled area of the electrets were covered with conductive electrode composites consisting of GNPs, CB and

PDMS (M_w = 139 kg·mol^{-1}) which were screen printed on both sides of the sample (Supporting information SI 2). The electrodes were 11 mm in diameter. A connective strip consisting of carbon black powder, going from the poled area to the sample edge, was applied on each side of the film, facing opposite edges. After mounting the sample in the tensile testing machine, the copper tape contacted the carbon black and a Keithley 2000 recorded the current passed through a Stanford Research Systems SR570 low noise current preamplifier while the sample was subjected to cyclic strains. Selected samples were subjected to further treatment in an oven set at 90 % relative humidity (RH) at 25 °C and at 85 °C, respectively, in order to asses their performance after exposure to different environments.

Results and Discussion

In this work, we used PZT particles with a diameter of 2 and 20 µm as a piezoelectric filler and two elastic PDMS matrices with different molar masses of 139 and 692 kDa. A schematic illustration of the preparation steps is depicted in Figure 1, while the reaction mechanism of tin-catalyzed cross-linking of PDMS is shown in the supporting information (SI 3). SEM micrographs show that the 2 µm sized particles have a mostly homogenous size distribution, while the 20 µm particles consist of large agglomerates of primary particles (Figure 2a,b). Size measurements conducted from the SEM micrographs concluded that the average size of those agglomerates was around 21 ± 6.5 µm similar to the size given by the supplier. Prior to the preparation of the composites, it was essential to subject the particles to surface treatment with HMDS to render them hydrophobic, thus enhancing their compatibility with the PDMS matrix.[29,30] Through the surface functionalization, the PZT particles could be dispersed more easily in toluene and did not sediment as fast as the untreated particles (Figure 2c).

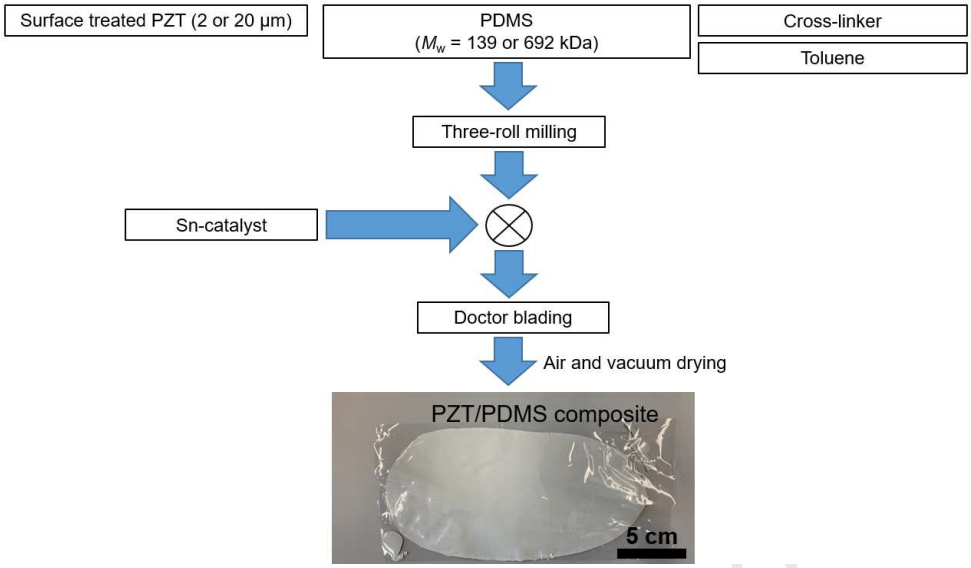

Figure 1: Schematic illustration of the preparation of PDMS composites with PZT particles.

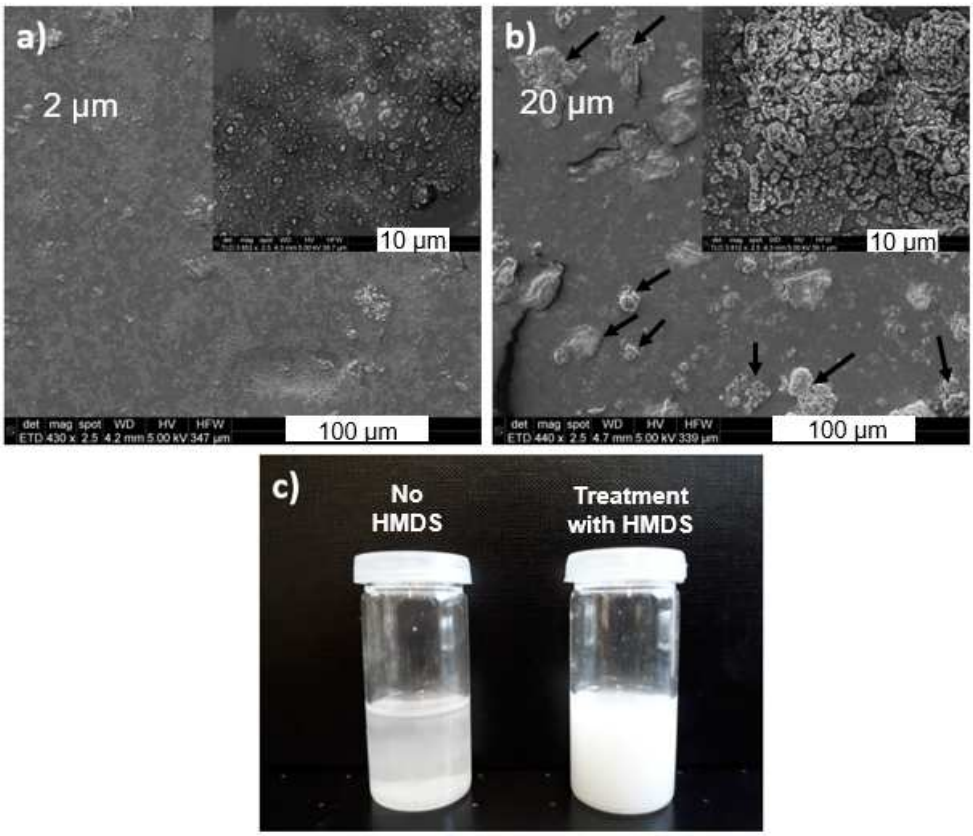

Figure 2. SEM micrographs of PZT particles with the average size of 2 (a) and 20 µm (b, some agglomerates of primary particles marked by arrows), and dispersion of PZT particles (2 µm) in toluene before (left) and after (right) surface functionalization with HMDS (c). The image was taken 5 min after the preparation of the dispersions.

The materials prepared as described in the experimental section are named as Ex[y-z], where x represents the mass of PDMS used in kDa, y the size of the particles used in μm, and z the vol.% of PZT filler. SEM micrographs of the resulting composites with different particle size and filler content are featured in Figure 3. The effective amount of filler dispersed in the PDMS was determined from the TGA measurements where the total filler content consisted of the residual mass after burning off the PDMS polymer (Figure 4). The vol.% of PZT particles within the composites was calculated using the densities of PZT (ρ=7.6 g/cm^3), of the cross-linker (ρ=0.98 g/cm^3) and that of PDMS (ρ=0.97 g/cm^3). Under inert atmosphere, the PDMS matrix should decompose without residual mass.[30] In general, the composites tendentially feature an enhancement in the thermal degradation stability with increasing filler content since they act as heat absorbants which is transferred to them from the polymer chains. Furthermore, the compatibilized particles also act as physical cross-linking centers for the PDMS chains through interfacial interactions which reinforce the material.[31] As a result, the temperature of maximum weight loss rate $T_{max,m}$ (*m* for major) of the main degradation step increased with the filler content. However, an increase of the filler content also hinders the chemical cross-linking reaction of polymers, and it was also reported that ceramics can act as catalysts, which promote the depolymerisation of PDMS at elevated temperatures.[32] Hence, $T_{max.m}$ decreased again towards lower temperatures at high filler content as observed for composites using both 2 and 20 μm PZT particles. In addition, a weak degradation step between 300 to 350 °C noted as the temperature of maximum weight loss rate $T_{max,w}$ (*w* for weak) appeared for composites with filler contents above 60 vol% although it was much weaker than $T_{max,s}$ which suggests the degradation of free polymer chains due to the inhibited chemical cross-linking reaction (Table 1).[33]

The composites prepared with PDMS 139k using 2 μm PZT exhibited higher thermal stability than the composites prepared with PDMS 692k with regards to $T_{max,m}$, likely due to the higher chemical cross-linking density of the former due to its lower molecular weight, which limits the thermally-induced segmental movement which was also supported by the increasing filler content that contributed to more physical cross-linking centres (Figure 4).[34] Higher molecular weight polymer composites exhibit an increased probability of random scission of polymer chains as a result of intramolecular and intermolecular redistribution reactions which leads to depolymerisation.[35] This trend is not observed with the composites utilizing 20 μm PZT particles since their total surface area is lower and therefore does not inhibit the cross-linking reaction between the polymer chains as heavily as in the case of 2 μm PZT particles. However, the lower surface area also leads to a decrease in their ability to effective-

ly act as physical cross-linking centers, and hence lower $T_{max,m}$ was overall observed for 20 µm PZT composites.[36]

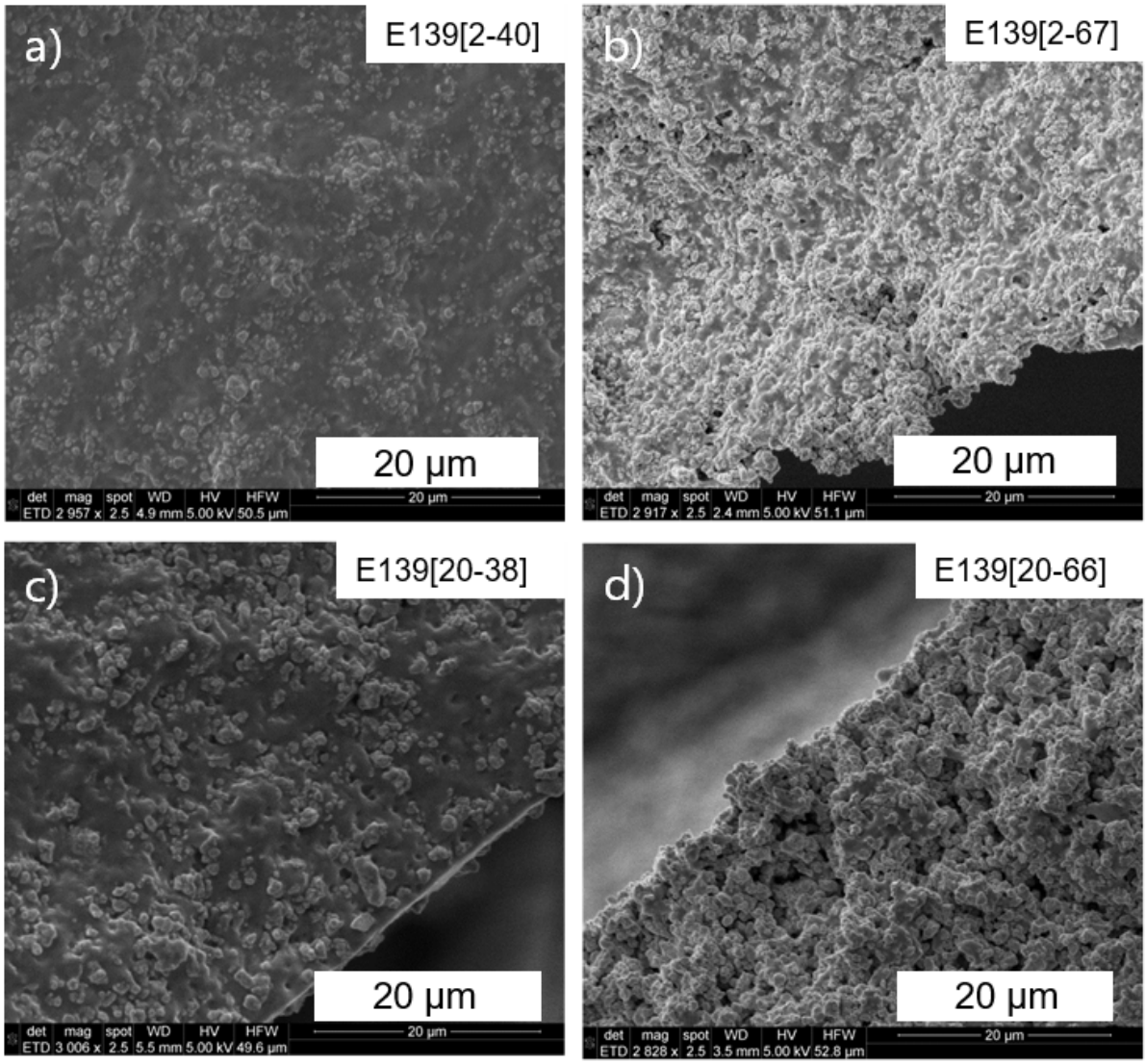

Figure 3. SEM micrographs of E139[2-40] (a), E139[2-67] (b), E139[20-38] (c) and of E139[20-66] (d), respectively.

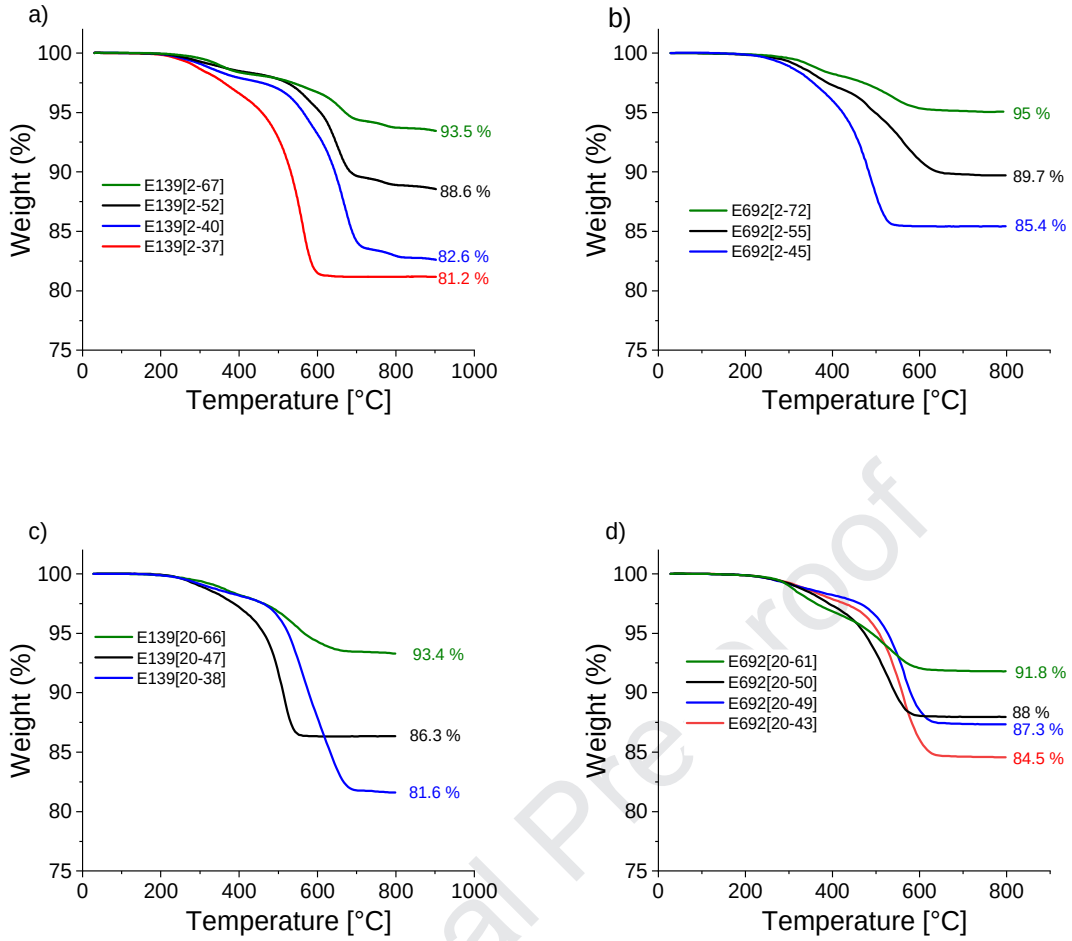

Figure 4. TGA curves of PDMS/PZT nanocomposites with different filler content: average particle size of PZT is 2 µm and PDMS 139k (a) and PDMS 692k (b) and average particle size of PZT is 20 µm and PDMS 139k (c) and PDMS 692k (d), respectively.

Table 1. Thermal properties of PDMS/PZT nanocomposites with PZT with an average particle size of 2 µm and 20 µm.

Sample	PZT [Vol%]	PDMS M_w [kg·mol^{-1}]	$T_{max,w}$ (°C)	$T_{max,m}$ (°C)
E139[2-37]	37.4	139	-	560
E139[2-40]	39.6	139	-	667
E139[2-52]	51.8	139	-	650
E139[2-67]	66.5	139	350	660
E692[2-45]	44.7	692	-	476
E692[2-55]	54.6	692	-	564
E692[2-72]	72.4	692	355	534
E139[20-38]	38	139	-	543
E139[20-47]	46.5	139	-	516
E139[20-66]	66.2	139	364	550
E692[20-43]	43	692	-	550
E692[20-49]	48.7	692	-	559
E692[20-50]	50.3	692	-	529
E692[20-61]	60.7	692	305	524

The composites exhibited an enhanced dielectric permittivity, which is attributed to the high ε' of PZT (ε' = 2'100). The increase in ε' was almost linear with increasing filler content (Figure

5, Table 2). Here, ε' seemed independent from both the particle size and the M_w of the PDMS matrix. For both particle sizes of PZT used, ε' values up to 34−35 were reached at a filler content of 66 vol. %. The obtained ε' values are in comparable range to PZT/PDMS composites reported earlier and are in good accordance to the model proposed by Yamada.[5] Although the filler content in the composites prepared in this work surpassed the percolation threshold, ε'did not register an abrupt increase since, despite the high ε' of the filler, PZT is not a conductive filler like metal particles which contribute to this phenomenon.[37,38] When the filler content exceeded 70 vol. %, ε' diminished due to the increased presence of air voids (ε' = 1) with higher filler content due to particle agglomeration.[37] The dielectric breakdown field, $E_{B,}$ decreased with increasing filler content and is influenced by the PDMS matrix used, an effect which has also been observed with other elastic matrices.[39] The composites containing PDMS 692k have a larger E_B than their lower molar mass counterparts. This can be explained by the fact that the longer polymer chains can fill in the voids within the material much better than shorter polymer chains and therefore disrupt the free-electron pathway, which is induced by the application of a voltage.[40] When using 2 µm PZT particles as filler, E_B decreased in a similar trend for composites using PDMS 139k and PDMS 692k, respectively, with the latter featuring a higher E_B at comparable filler content as explained earlier. For the composites using 20 µm PZT particles, the E_B of the composites with PDMS 139k was lower compared to the corresponding composites with 2 µm PZT particles, while the E_B of the PDMS 692k composites were comparable in magnitude at a filler content of ≤ 50 vol.%. These observations support the argument that the particle-polymer interface layers are reduced with increasing particle size due to the reduction of the particle surface area which explains the lower E_B for 20 µm PZT particles. With increasing M_w of the PDMS, however, this effect diminished as seen in Figure 5 although it declined rapidly with the filler content for the 20 µm PZT composites. The E_B values exhibited large deviations due to the presence of localized defects within the material as a result of agglomerate formation through the relatively high filler content but the distribution of values narrows down after 50 vol.% where the E_B decreased even further as adjacent particle become more interconnected with each other.

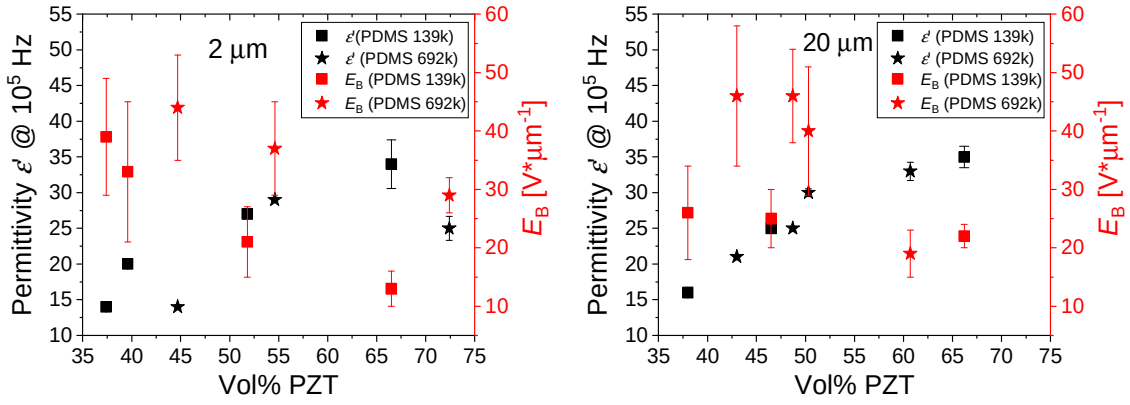

Figure 5. Permittivity ε' and breakdown field E_B of PZT/PDMS nanocomposites with an average particle size of 2 and 20 µm in PDMS 139k and 692k matrices.

Table 2. Summary of dielectric permittivity at 10^5 Hz and dielectric breakdown field of PDMS/PZT nanocomposites with PZT with an average particle size of 2 µm and 20 µm.

Sample	PZT [Vol%]	PDMS M_w [kg·mol^{-1}]	Permittivity ε'@ 10^5 Hz	E_B [V·µm^{-1}]
E139[2-37]	37.4	139	14 ± 0.2	39 ± 10
E139[2-40]	39.6	139	20 ± 0.3	33 ± 12
E139[2-52]	51.8	139	27 ± 0.7	21 ± 6
E139[2-67]	66.5	139	34 ± 3.4	13 ± 3
E692[2-45]	44.7	692	14 ± 0.3	44 ± 9
E692[2-55]	54.6	692	29 ± 0.2	37 ± 8
E692[2-72]	72.4	692	25 ± 1.7	29 ± 3
E139[20-38]	38	139	16 ± 0.2	26 ± 8
E139[20-47]	46.5	139	25 ± 0.2	25 ± 5
E139[20-66]	66.2	139	35 ± 1.5	22 ± 2
E692[20-43]	43	692	21 ± 0.1	46 ± 12
E692[20-49]	48.7	692	25 ± 0.2	46 ± 8
E692[20-50]	50.3	692	30 ± 0.5	40 ± 11
E692[20-61]	60.7	692	33 ± 1.3	19 ± 4

The composites were also subjected to mechanical tensile testing (Supporting information SI 4 and 5). With increasing filler content, the strain at break values for composites PDMS 139k decreased due to the increasing brittleness of the materials (Figure 6, Table 3). There seemed to be no substantial difference between the smaller and larger particles in terms of the Young's modulus *Y* and the strain at break values although the difference in *Y* and strain at breakvalues manifested itself at larger filler content. By using PDMS 692k instead of PDMS 139k, the strain at break value was enhanced due to the higher flexibility of the polymer chains. For composites using both 2 µm and 20 µm PZT particles dispersed in both PDMS 139k and 692k, respectively, *Y* increased initially with the filler content due to the reinforcing effect of the filler as additional physical cross-linking agents. As the surface-to-volume ratio was higher for the 2 µm particles, the resulting *Y* values were higher than for the 20 µm PZT composites. However, a decrease in *Y* at high filler contents (50 vol% or above) was observed

due to the increasing agglomeration of particles with rising filler content and the subsequent dewetting of the polymer at the polymer/particle interphase (Table 3, Entries 3 and 4, 6 and 7, 9 and 10, 12 and 13).[41,42] As a result, the reinforcing effect of the particles diminished due to the reduction of the polymer/particle interactions, and hence the mechanical properties deteriorated which was manifested in both the reduction of *Y* and the strain at break value. Below a filler content of 50%, the 20 µm PZT/PDMS composites for PDMS 692k at filler contents showcased a higher strain at break value which indicated that the chemical cross-linking was less hindered and the polymer chains less entangled compared to the scenario where the smaller PZT particles are used as filler where the latter limits the diffusion of the polymer chains and act as physical cross-linkers.

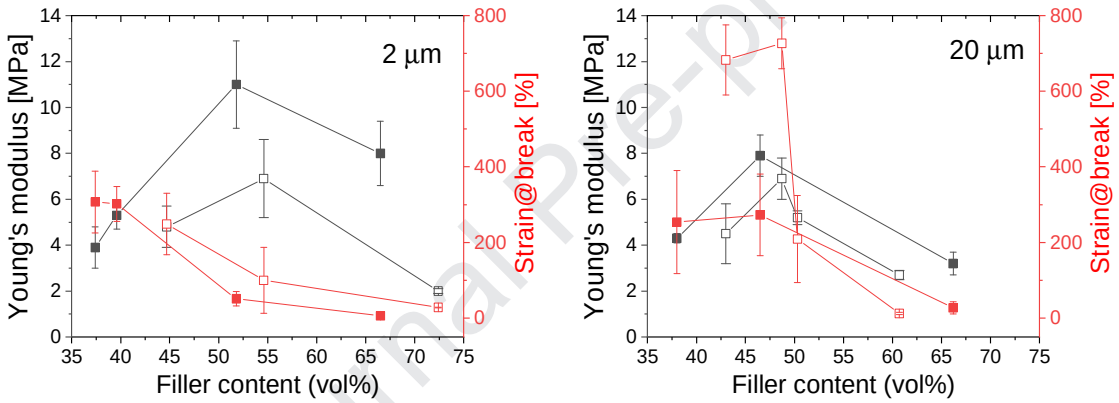

Figure 6. Young's modulus *Y* and strain-at-break values of composites consisting of 2 µm (left) and 20 µm (right) PZT particles using PDMS 139k (filled symbols) or 692k (empty symbols) as polymer matrix.

Table 3. Summary of the mechanical properties of PDMS/PZT nanocomposites.

Sample	PZT [Vol%]	PDMS M_w [kg·mol^{-1}]	$Y_{10\%}$ [MPa]	Maximum strain @ break [%]
E139[2-37]	37.4	139	3.9 ± 0.9	307 ± 82
E139[2-40]	39.6	139	5.3 ± 0.6	302 ± 46
E139[2-52]	51.8	139	11 ± 1.9	51 ± 19
E139[2-67]	66.5	139	8 ± 1.4	5.9 ± 1.2
E692[2-45]	44.7	692	4.8 ± 0.9	249 ± 81
E692[2-55]	54.6	692	6.9 ± 1.7	100 ± 87
E692[2-72]	72.4	692	2.0 ± 0.1	28 ± 0.8
E139[20-38]	38	139	4.3 ± 0.2	254 ± 136
E139[20-47]	46.5	139	7.9 ± 0.9	273 ± 108
E139[20-66]	66.2	139	3.2 ± 0.5	27 ± 16
E692[20-43]	43	692	4.5 ± 1.3	683 ± 93
E692[20-49]	48.7	692	6.9 ± 0.9	727 ± 67
E692[20-50]	50.3	692	5.2 ± 0.3	209 ± 115
E692[20-61]	60.7	692	2.7 ± 0.2	12 ± 3.2

DMA measurements performed on selected composites with roughly the similar filler content revealed a constant storage modulus, *E'*, from 0 to 1 Hz. It has to be mentioned that composites with higher filler content were not suitable for this characterization due to their increasing brittle nature. In general the storage modulus increased with the amount of filler, which is indicative of the reinforcing character of the filler thus contributing to the stiffness of the material (Figure 7). The increase in the filler amount is associated with an increase in the particle surface area and in the resulting polymer/particle interface.[43] Hence, the loss modulus also increased since the reinforcement of PDMS with the filler required a larger force to induce the same stress. With increasing frequency, a decline in the modulus was observed, which could be due to the diminishing entanglements between the particles and the polymer chains. A steeper decline in the loss modulus, *E''*, is observed for the composites using PDMS 692k since the cross-linking density is lower compared to the composites using PDMS 139k, thus giving rise to softer and more flexible materials.[44]

Both composites E139[2-52] and E692[20-50] are materials where the adjacent particles start to become more interconnected with each other as a result of the growing filler content. The increase in the frequency led to the separation of the interconnected particles, and hence the polymer/particle interface area increased. In the case of E139[2-52], the increase in the polymer/particle interface led to a brief increase in both the storage modulus *E'* and the loss modulus *E''* due to the destruction of the particle agglomerates and the ensuing activity of the resulting isolated particles as physical cross-linkers. This phenomenon was not observed for E692[20-50] where the increase in the polymer-particle interface area was smaller due to the lower surface-to-volume ratio of the 20 μm PZT particles and therefore had a lower positive impact on the mechanical properties of the corresponding composites in comparison to 2 μm PZT particles. Therefore, the initial increase in frequency led to decline in both *E'* and *E''*.

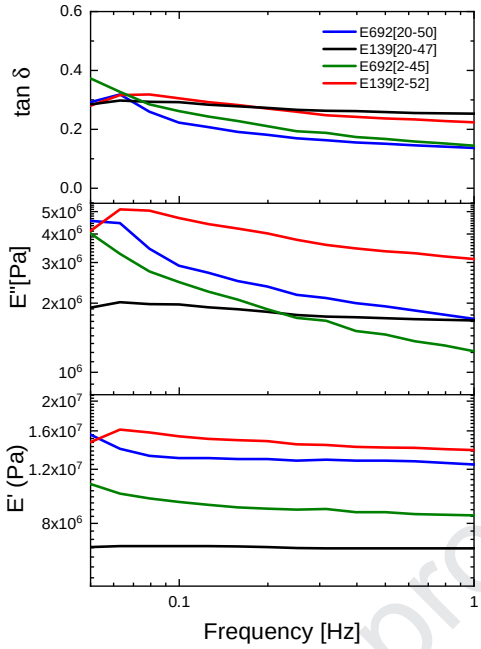

Figure 7. DMA graphs showing the storage modulus *E'*, loss modulus *E''* and loss factor *tan δ* of selected PZT/PDMS composite materials containing roughly the same filler content with varying filler size and molecular weight of the PDMS matrix.

The goal of dispersing PZT into PDMS was to produce flexible and stretchable piezoelectric materials. However, the formed composites consist of randomly oriented dispersed ceramic particles and thus no macroscopic piezoelectric response was expected.[26] To achieve a macroscopic electromechanical response, the composites were poled at elevated temperatures and high electric fields. Previous reports showed optimized poling conditions of ferroelectric-PDMS composites at 100−150 °C and 2−7.5 $V \cdot \mu m^{-1}$.[23,45,46] As expected, under the same poling conditions (12 $V \cdot \mu m^{-1}$ at 150 °C), an increase in the d^*_{33} piezoelectric coefficient with increasing filler content was observed. For instance, composites E139[2-z] showed an increase of d^*_{33} from 2.7 to 7.8 $pC \cdot N^{-1}$, when the filler content increased from 37 to 52 vol.% (Table 4, Entries 1−3). It is well known for composites that elevated temperature and higher electric field results in a higher piezoelectric constant (due to a higher mobility of dipole movement of the ferroelectric filler), on the other hand the maximum temperature is limited by the melting point and decomposition temperature of the polymer. Furthermore the maximum allowed electric field (E) is determined by the dielectric strength of the material (E_b), where $E < E_b$, and further decreases with increasing temperature. Therefore, some of the different composites were polarized using different conditions. The breakdown field, E_B, is reduced with increasing filler content due to particle agglomeration as explained earlier. Since the E_B of the composite E139[2-67] was at 13 $V \cdot \mu m^{-1}$, poling at 12 $V \cdot \mu m^{-1}$ was quite risky in

terms of inducing dielectric breakdown. Therefore, E139[2-67] was poled at 6 $V \cdot \mu m^{-1}$ at a temperature of 155 °C instead. As a result, this composite exhibited a d^*_{33} of 22.7 $pC \cdot N^{-1}$ (Figure 8, Table 4, Entry 5). Increasing the molecular weight of the PDMS matrix allowed the incorporation of more filler, while the dielectric breakdown field was enhanced. Therefore, a composite E692[2-72] could be prepared and poled at 12 $V \cdot \mu m^{-1}$. However, it was difficult to remove it from the electrodes after poling at 150 °C since it easily broke apart during the removal because of its brittleness. To overcome this problem, the poling temperature was reduced to 100 °C, which enabled a facile removal of the sample from the electrodes after poling. The piezoelectric response of this poled composite was d^*_{33} = 30 $pC \cdot N^{-1}$. With this composite, it has also been illustrated that the poling temperature increased the d^*_{33} of the resulting composite, which is in agreement with the literature.[47] For instance, when E692[2-72] was poled at an electric poling field of 12 $V \cdot \mu m^{-1}$ and the temperature was increased from 24 °C to 159 °C, the d^*_{33} coefficients increased from 20.5 to 30 $pC \cdot N^{-1}$ (Table 4, Figure 8, Entries 10 and 11).

Aside from the poling temperature, the electric field with which the composites are poled also has an impact on the d^*_{33}. The increase in the electric field leads to an enhancement in the d_{33} as shown by E139[2-67] where an increase of the d^*_{33} from 15.8 to 22.7 $pC \cdot N^{-1}$ was observed when the electric field was increased from 3 to 6 $V \cdot \mu m^{-1}$ at 155 °C to 159 °C (Table 4, Entries 4 and 5). In direct comparison, E139[20-66] with larger particles exhibited a d^*_{33} = 40 $pC \cdot N^{-1}$ when poled at 159 °C and 12 $V \cdot \mu m^{-1}$ (Figure 8, Table 4). This is in line with previous reports which stated that the d^*_{33} increases with the particle size in PZT composites.[25,46]

In comparison to the permittivity ε' which featured a linear increase with filler content, d^*_{33} values were quite small until 30 vol.% which corresponds to the percolation threshold for isotropically dispersed particles.[37] Therefore, d^*_{33} exhibited a significant increase above the percolation threshold as the composites experience a transition from a 0−3 to 1−3 composite where adjacent particles became interconnected (Figure 3).[5] The 20 μm PZT composites showcased higher d^*_{33} since there are less polymer/particle multilayers along the film thickness due to the larger particle size, therefore stress is more effectively transferred between the PZT domains.

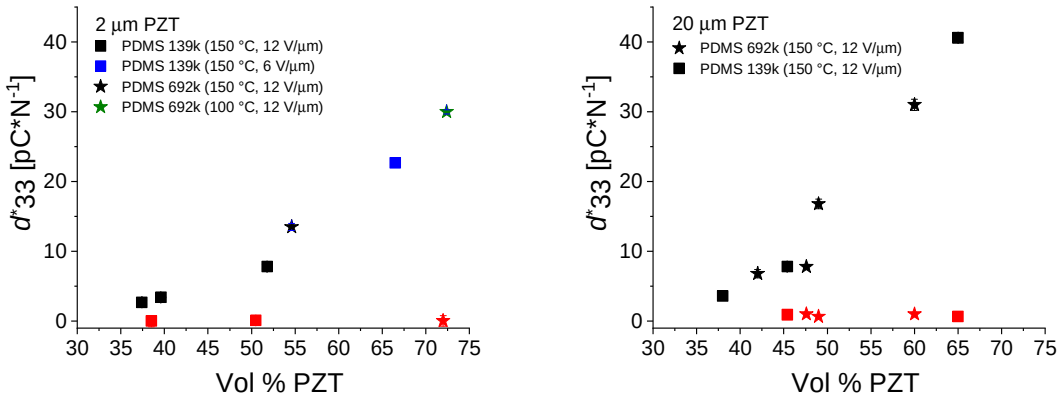

Figure 8. Longitudinal piezoelectric coefficient d^*_{33} of various composites containing PZT with a particle size of 2 µm (left) and a particle size of 20 µm (right), poled at different conditions. Non-poled reference samples using PDMS 139k (square) and 692k (star) are illustrated in red color.

Table 4. Summary of d^*_{33} piezoelectric coefficient of PDMS/PZT nanocomposites measured at a force of 0.6 N and the d^*_{31} piezoelectric coefficient for selected samples.

Entry	Sample	PDMS M_w [kg·mol^{-1}]	PZT [Vol%]	Poling T [°C]	Poling field [V/µm]	d^*_{33} [pC·N^{-1}][a]	d^*_{31} @25 % strain [pC·N^{-1}][a]
1	E139[2-37]	139	37.4	159	12	2.7	16
2	E139[2-40]	139	39.6	155	12	3.5	26
3	E139[2-52]	139	51.8	150	12	7.8	-
4	E139[2-67]	139	66.5	159	3	15.8	-
5	E139[2-67]	139	66.5	155	6	22.7	-
6	E139[2-67]	139	66.5	109	6	20	-
7	E692[2-55]	692	54.6	159	12	13.5	-
8	E692[2-55]	692	54.6	153	18	14	-
9	E692[2-55]	692	54.6	99	12	16.1	-
10	E692[2-72]	692	72.4	159	12	30	-
11	E692[2-72]	692	72.4	23.6	12	20.5	-
12	E139[20-38]	139	38	145	12	3.6	30
13	E139[20-47]	139	46.5	25	12	7.8	-
14	E139[20-47]	139	46.5	151	12	9	-
15	E139[20-47]	139	46.5	151	12	7.2	-
16	E139[20-47]	139	46.5	149	18	6	-
17	E139[20-66]	139	66.2	25	12	33	-
18	E139[20-66]	139	66.2	101	6	35	-
19	E139[20-66]	139	66.2	101	12	35	-
20	E139[20-66]	139	66.2	159	12	40	-
21	E139[20-66]	139	66.2	25	12	34	-
22	E692[20-43]	692	43	149	12	6.8	48
23	E692[20-49]	692	48.7	150	12	7.8	-
24	E692[20-50]	692	50.3	104	12	13	-
25	E692[20-61]	692	60.7	25	12	23	-
26	E692[20-61]	692	60.7	100	6	27	-

[a]Electrodes where screen printed on two opposite surfaces prior to poling

Apart from d^*_{33}, the d^*_{31} piezoelectric coefficient was also measured in this study. The force acting on the composites during the d^*_{33} measurements is parallel to the electric field applied during poling, while the applied force during the d^*_{31} measurement is perpendicular to the pol-

ing direction. The experimental setup used for the d^*_{31} measurement was described in a previous report by Ko *et al.* (Supporting information SI 6).[11] Similar to the d^*_{33}, the d^*_{31} piezoelectric coefficient of composites with similar filler content, poling conditions and identical strains increased with the PZT particle size. The difference in the performance of the two composites E139[2-37] and E139[20-38] can be seen in the generated charges and voltages (Figure 9). The cyclic strain measurements conducted for the composites using the 2 μm at 25 % strain and at a frequency of 0.1 Hz led to an output of 1.58 V or 0.9 nC which corresponded to a d^*_{31} of 16 $pC \cdot N^{-1}$ (Figure 9a-c) with a tensile force of 2.9 N acting on the E139[2-37]. When E139[20-38] was subjected to the same measurements, the voltage generated from the cyclic measurements at the same strain and frequency increased from 1.58 V to 2.3 V, with the latter voltage corresponding to generated charges of 1.25 nC and a d^*_{31} value of 30 $pC \cdot N^{-1}$, as a result of increasing the PZT particle size from 2 to 20 μm. The corresponding tensile force to strain E139[20-38] was 3.02 N. The larger output exhibited by the composites with 20 μm PZT particles composed of agglomerates of primary PZT particles is attributed to the higher connectivity between the particles due to the shorter interparticle distance. [48] The reduced interface area between the particle and the polymer associated with the increase in the size of the particle leads to less imperfections in the joining the particles.[49] In short, different stresses act on the PZT particles depending on their size, and in the case of 20 μm PZT particles the shorter interparticle distance between the primary particles within the agglomerates lead to a higher stress at the contact point between particles.[17,18] Hence, the positive correlation between stress and piezoelectric properties is reflected in the higher d^*_{33} and d^*_{31} values for the composites using the 20 μm PZT particles.

The long-term reliability of the films were confirmed since the generated charges remained within the similar regime when assessing the performance at different time intervals (Figure 9a and d). Furthermore, composites containing 20 μm PZT particles dispersed in PDMS 692k were also subjected to d^*_{31} measurements at similar filler content (43 vol.%) in order to determine the effect of the polymer matrix (Figure 10). Due to the increase in structural defects with increasing filler content caused by partice agglomeration, composites with filler content above 50 vol.% could not be investigated for the performed d^*_{31} measurements. For the synthesis of E692[20-43] more toluene had to be used, hence the formulated films were thinner than the composites with PDMS 139k using the same amounts of reagents. The presence of defects in the PDMS 692k composites could lead to a higher rupture probability, therefore the films were initially stretched to 15% strain, which yielded a d^*_{31} of ~ 40 $pC \cdot N^{-1}$ from an output voltage of 1.96 V (Figure 10a and c) and a charge of 0.91 nC at a force of 1.23 N. When

the film was stretched to 25%, the generated d^*_{31} surpassed 40 pC·N^{-1} and the output voltage of 3.08 V, the charge of 2.11 nC at a force of 1.87 N was obtained. Unfortunately, the film experienced rupture after a few days of measurement (Figure 10b and d). As shown earlier the PDMS 692k matrix reduced the Young's modulus of the composite materials compared to PDMS 139k matrix, which should lead to an increase of output current and hence also a larger d^*_{31} coefficient since a higher stress acts between adjacent particles due to the more efficient stress transfer to the particles from the external source.[18] As can be seen from the measurement the d^*_{31} coefficient increased from 30 to to 48 pC·N^{-1} by changing the matrix from PDMS 139k to PDMS 692k. This renders it more beneficial for applications because higher output currents can be generated, or less input force is needed. The results obtained for the d^*_{31} are higher as compared to d^*_{33}, which is usually not the case. We assume that the capacitor effect related to the change in charge densities of the composites plays a major role. Furthermore, the force to generate the desired strains are higher than the strains to which the composites were subjected to during the d^*_{33} measurements. During cycling the thickness of the composite films will change, which affects the interparticle distance as mentioned earlier since they were incorporated within the composites alone through physical cross-linking. Hence, a difference in the charge density will occur.

Although the generated voltages are comparable to the output of other PZT composites, the higher strains which can be generated with the composites featured in this work expand their potential as dielectric elastomers used to generate electricity.[50,51]

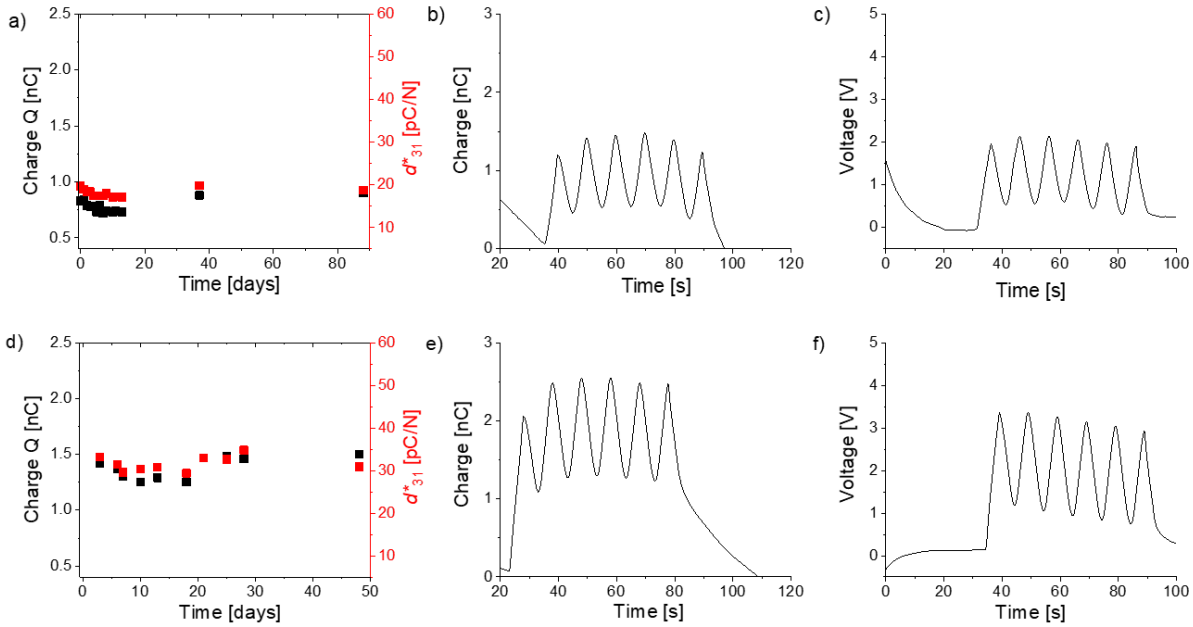

Figure 9. The d^*_{31} and charges generated by E139[2-37] at a strain of 25 %, the generated charges and voltage from 5 cycles when the sample was strained by 25% at 0.1 Hz, 88 days after poling (top row) and d_{31} and charges generated by E139[20-38] at a strain of 25 % and the generated charges and voltage from 6 cycles when the sample was strained by 25% at 0.1 Hz, 10 days or 225 h after poling (bottom row).

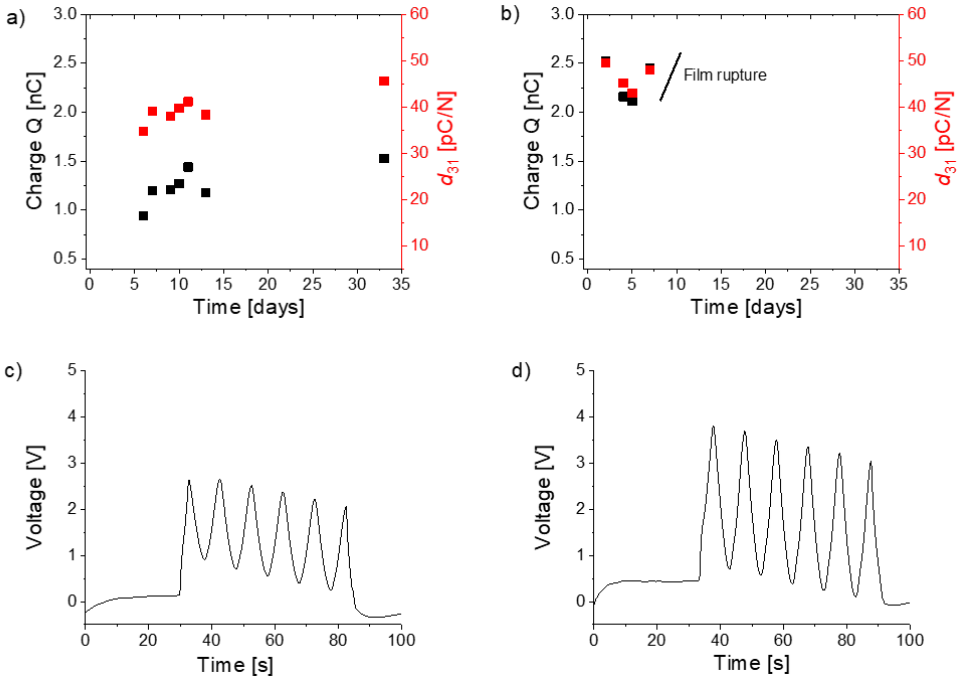

Figure 10. The d^*_{31} and charges generated by E692[20-43] at a strain of 15 (a) and 25 % (b) (top row). The generated voltages at 15% (c) and 25% (d) strain from a measurement of 5 cycles conducted after 6 (c) and 5 days (d) after poling, respectively, are depicted in the bottom.

The effect of the environment on the material performance was also investigated for selected composites. After exposure to 90% relative humidity (RH) for 24 hours, the d^*_{31} of E139[2-40], at a strain of 25 %, was altered from 30 to 36 pC·N^{-1}, which corresponded to a change in the charge from 1.92 nC to 1.8 nC. The material softened after this treatment, therefore the d^*_{31} increased despite the reduction in the generated charge. The exposure of E139[2-37] to 80 °C for the same period of time saw the d^*_{31} slightly change from 18.2 to 20.5 pC·N^{-1} and a change in the charge from 0.97 nC to 1.09 nC (Figure 11). Thus, it has been found that such composites have not shown any major changes in their piezoelectric d^*_{31} coefficients especially at enhanced temperatures below T_c thus indicating their ability to be used under those selected environmental conditions.

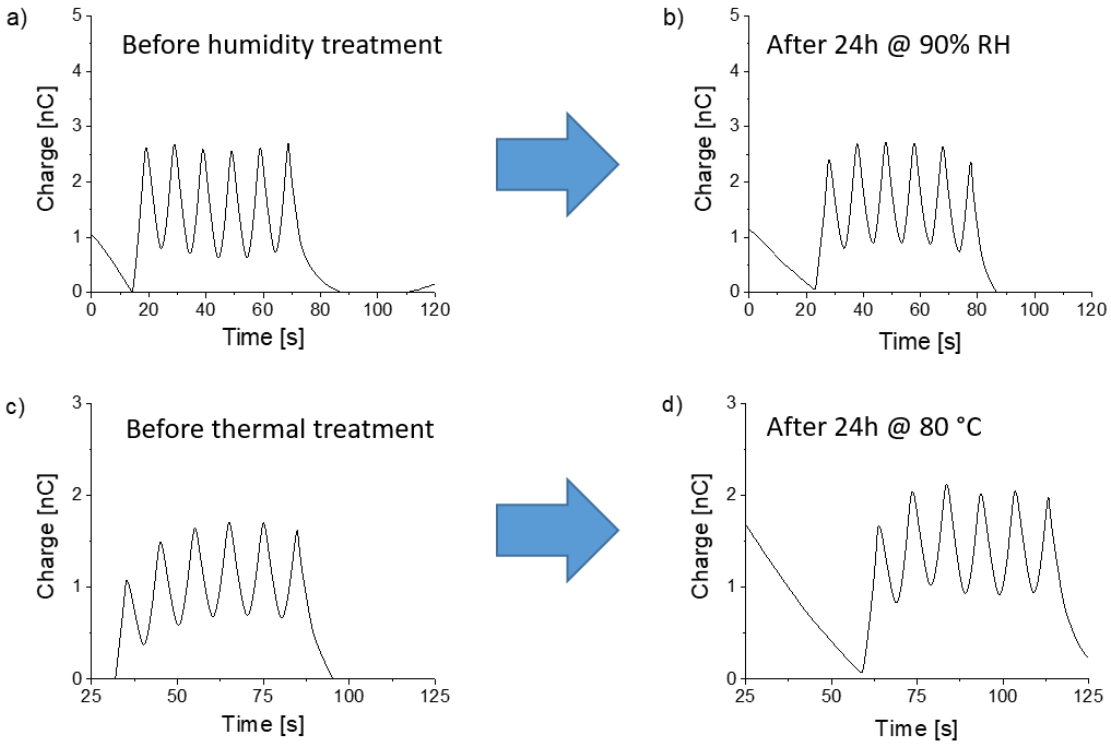

Figure 11. Generated charges of E139[2-40](a,b) and E139[2-37](c,d) before and after humidity and thermal treatment, respectively.

Composite E139[20-38] generated a voltage of 2.3 V when stretched by 25% and has been found to exhibit the best compromise between piezoelectric performance and mechanical flexibility and stability. To demonstrate the potential of the newly developed material for applications, a demonstrator consisting of a clamping/contact device and a measuring device with LCD display was constructed (Figure 12). The piezoelectric film sensor is clamped in the contact device and contacted via two circuit boards on the front and back, which con-

nect the sensor to the measuring device via cables. The sensor signal is amplified and filtered in the measuring device using a "voltage mode amplifier". Then the signal is digitized with the ADC. The first line from the LCD shows the signal curve and in the second line the current peak value is recorded for a few seconds. The average offset voltage of the measuring circuit has already been subtracted from the peak value. Only the positive signal deflection is taken into account in the measurement. With the voltage amplitude, the signal influence by the deformation of the piezo film can be compared and assessed. In the present device, the piezo film signal is loaded with 500 kΩ and then amplified with 20 V. The measured value full scale (0023) corresponds to an amplitude of about 165 mV of the piezo film. For example, a displayed value of 100 corresponds to a voltage of 16 mV on the piezo with a load of 500 kΩ. Figure 12 shows how the mechanical stress induced by pressing a plastic knob by a finger generates an electrical signal, which is detected by the black electronic device.

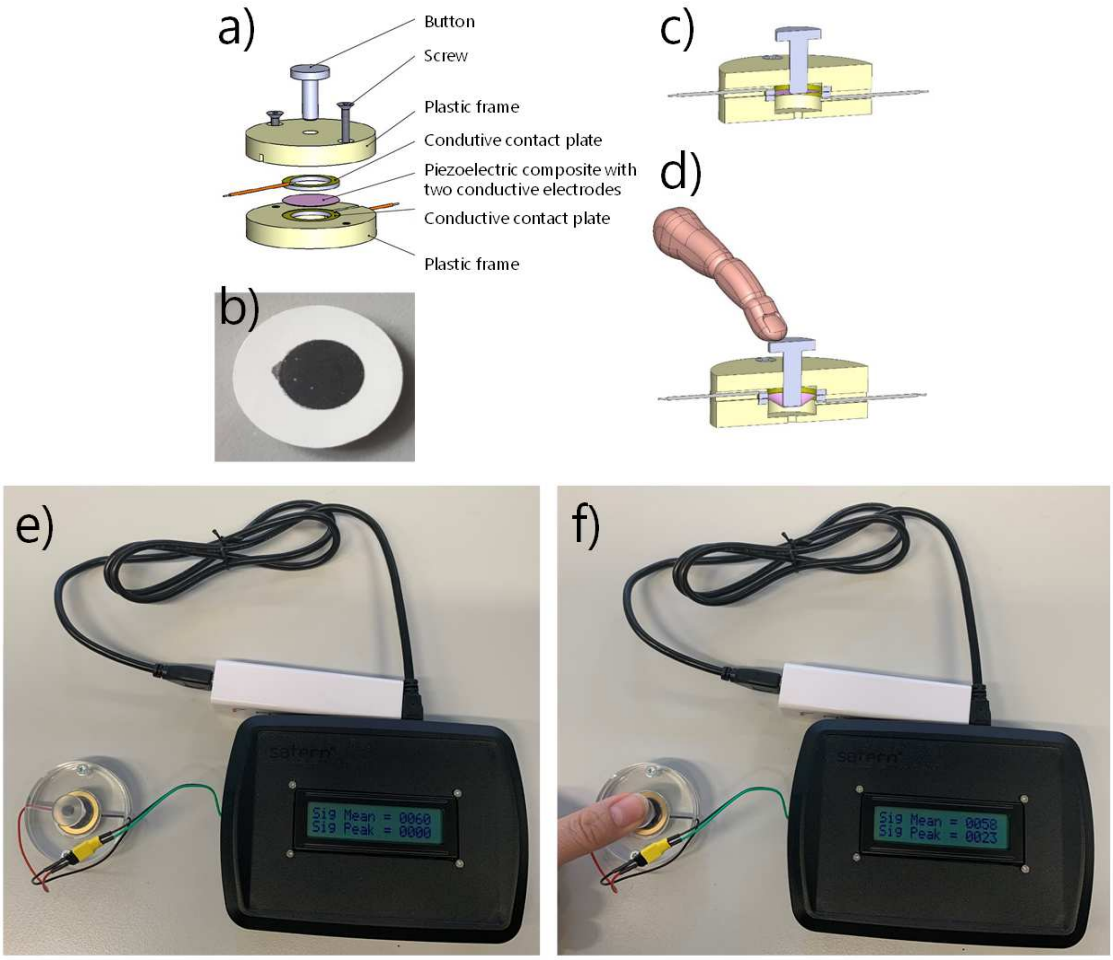

Figure 12. The components used for the construction of press sensor (a), photograph of the piezoelectric film with black conductive films on top and bottom (b), schematic representation of the press sensor in the relaxed (c) and press state (d) as well as the photograph of the sensor and the electronic de-

vice used to monitor the generated electrical signal. A change in the Sig Peak from 0 to 0.023 can be seen for the relaxed (e) and pressed sensor (f).

Conclusions

Flexible PZT/PDMS composite films with a thickness of 120−250 μm were prepared, starting from two PDMS matrices of different molar mass and surface functionalized PZT particles of 2 μm and 20 μm. Elastic composites with a large content of filler were successfully prepared by the doctor blading technique. They were poled in a strong electric field at elevated temperature in order to induce a remanent polarization of the ferroelectric particles responsible for the macroscopic piezoelectric response. The poled composites containing 20 μm particles produced larger piezoelectric response coefficients (both d^*_{31} and d^*_{33}) than the composites using 2 μm PZT particles at similar filler content. The potential of the most promising composite in a press sensor was demonstrated. Because of the good elastic and piezoelectric properties these materials are highly attractive for applications in sensing, energy harvesting, and stretchable electronics.

CRediT authorship contribution statement

Jose Enrico Q. Quinsaat: Investigation, Methodology, Formal analysis, Writing-original draft. **Tym de Wild:** Formal analysis, Writing-review & editing. **Frank A. Nüesch:** Funding acquisition, Supervision, Writing-review and editing. **Dragan Damjanovic:** Writing-review & editing. **Ronny Krämer:** Investigation, Formal analysis. **Georg Schürch:** Investigation, Formal analysis**. Daniel Häfliger:** Funding acquisition, Supervision. **Frank Clemens:** Writing-review & editing. **Tutu Sebastian:** Writing-review & editing. **Mihaela Dascalu:** Investigation, Formal analysis, Writing-review & editing. **Dorina M. Opris:** Funding acquisition, Supervision, Investigation, Formal analysis, Writing-original draft.

Declaration of competing interest

The authors declare that they have no known competing financial interests or personal relationships that could have appeared to influence the work reported in this paper.

Acknowledgements

We would like to thank Mrs. Beatrice Fischer for the TGA measurements, Dr. Yee Song Ko

for useful discussions, Mr. Yauhen Sheima for providing the images of the set-up and Dr. Philip Caspari for the DMA measurements (all Empa). We would also like to extend our gratitude to the Swiss Federal Laboratories for Materials Science and Technology (Empa) for providing the infrastructure for this work.

This project was financially supported by Innosuisse [25368.1] and the Swiss National Science Foundation SNSF [IZSAZ2_173358].

References

[1] Ali D, Yu B, Duan X, Yu H, Zhu M. Enhancement of output performance through post-poling technique on $BaTiO_3$/PDMS-based triboelectric nanogenerator. Nanotechnology 2017;28. https://doi.org/10.1088/1361-6528/aa52b7.

[2] Xie M, Zhang Y, Kraśny MJ, Bowen C, Khanbareh H, Gathercole N. Flexible and active self-powered pressure, shear sensors based on freeze casting ceramic-polymer composites. Energy Environ Sci 2018;11:2919–27. https://doi.org/10.1039/c8ee01551a.

[3] Zheng P, Zhang JL, Tan YQ, Wang CL. Grain-size effects on dielectric and piezoelectric properties of poled BaTiO3ceramics. Acta Mater 2012;60:5022–30. https://doi.org/10.1016/j.actamat.2012.06.015.

[4] Ehrhardt C, Fettkenhauer C, Glenneberg J, Münchgesang W, Pientschke C, Großmann T, et al. BaTiO3-P(VDF-HFP) nanocomposite dielectrics - Influence of surface modification and dispersion additives. Mater Sci Eng B Solid-State Mater Adv Technol 2013;178:881–8. https://doi.org/10.1016/j.mseb.2013.04.013.

[5] Babu I, de With G. Highly flexible piezoelectric 0-3 PZT-PDMS composites with high filler content. Compos Sci Technol 2014;91:91–7. https://doi.org/10.1016/j.compscitech.2013.11.027.

[6] Babu I, Van Den Ende DA, De With G. Processing and characterization of piezoelectric 0-3 PZT/LCT/PA composites. J Phys D Appl Phys 2010;43. https://doi.org/10.1088/0022-3727/43/42/425402.

[7] Bernard F, Gimeno L, Viala B, Gusarov B, Cugat O. Direct Piezoelectric Coefficient Measurements of PVDF and PLLA under Controlled Strain and Stress. Proceedings 2017;1:335. https://doi.org/10.3390/proceedings1040335.

[8] Rianyoi R, Potong R, Ngamjarurojana A, Chaipanich A. Poling effects and piezoelectric properties of PVDF-modified 0–3 connectivity cement-based/lead-free 0.94(Bi0.5Na0.5)TiO3–0.06BaTiO3piezoelectric ceramic composites. J Mater Sci

2018;53:345–55. https://doi.org/10.1007/s10853-017-1533-4.

[9] Ting Y, Gunawan H, Sugondo A, Chiu CW. A new approach of polyvinylidene fluoride (PVDF) poling method for higher electric response. Ferroelectrics 2013;446:28–38. https://doi.org/10.1080/00150193.2013.820983.

[10] Ko YS, Nüesch FA, Damjanovic D, Opris DM. An All-Organic Elastomeric Electret Composite. Adv Mater 2017;29:1–6. https://doi.org/10.1002/adma.201603813.

[11] Ko YS, Nüesch FA, Opris DM. Charge generation by ultra-stretchable elastomeric electrets. J Mater Chem C 2017;5:1826–35. https://doi.org/10.1039/c6tc04956g.

[12] Zhang Y, Xie M, Roscow J, Bao Y, Zhou K, Zhang D, et al. Enhanced pyroelectric and piezoelectric properties of PZT with aligned porosity for energy harvesting applications. J Mater Chem A 2017;5:6569–80. https://doi.org/10.1039/C7TA00967D.

[13] Bele A, Cazacu M, Stiubianu G, Vlad S, Ignat M. Polydimethylsiloxane–barium titanate composites: Preparation and evaluation of the morphology, moisture, thermal, mechanical and dielectric behavior. Compos Part B Eng 2015;68:237–45. https://doi.org/10.1016/j.compositesb.2014.08.050.

[14] Yoshiyama K, Mori M, Hagiwara M, Fujihara S. Effect of particle size and morphology on the performance of BiFeO3–PDMS piezoelectric generators. CrystEngComm 2020;22:2919–25. https://doi.org/10.1039/D0CE00067A.

[15] Sebastian T, Lusiola T, Clemens F. Ferroelectric hybrid fibers to develop flexible sensors for shape sensing of smart textiles and soft condensed matter bodies. Smart Mater Struct 2017;26:1–11. https://doi.org/10.1088/1361-665X/aa5bd2.

[16] Pelrine R, Kornbluh RD, Eckerle J, Jeuck P, Oh S, Pei Q, et al. Dielectric Elastomers: Generator Mode Fundamental Applications. SPIE's 8th Annu Int Symp Smart Struct Mater 2001;4329:148–56. https://doi.org/10.1117/12.432640.

[17] Chou X, Zhu J, Qian S, Niu X, Qian J, Hou X, et al. All-in-one filler-elastomer-based high-performance stretchable piezoelectric nanogenerator for kinetic energy harvesting and self-powered motion monitoring. Nano Energy 2018;53:550–8. https://doi.org/https://doi.org/10.1016/j.nanoen.2018.09.006.

[18] Niu X, Jia W, Qian S, Zhu J, Zhang J, Hou X, et al. High-Performance PZT-Based Stretchable Piezoelectric Nanogenerator. ACS Sustain Chem Eng 2019;7:979–85. https://doi.org/10.1021/acssuschemeng.8b04627.

[19] Kim DH, Shin HJ, Lee H, Jeong CK, Park H, Hwang G-T, et al. In Vivo Self-Powered

Wireless Transmission Using Biocompatible Flexible Energy Harvesters. Adv Funct Mater 2017;27:1700341. https://doi.org/10.1002/adfm.201700341.

[20] Li Z, Zhu G, Yang R, Wang AC, Wang ZL. Muscle-Driven In Vivo Nanogenerator. Adv Mater 2010;22:2534–7. https://doi.org/10.1002/adma.200904355.

[21] Shi B, Li Z, Fan Y. Implantable Energy-Harvesting Devices. Adv Mater 2018;30:1801511. https://doi.org/10.1002/adma.201801511.

[22] Babu I, de With G. Enhanced electromechanical properties of piezoelectric thin flexible films. Compos Sci Technol 2014;104:74–80. https://doi.org/10.1016/j.compscitech.2014.08.022.

[23] Babu I, Hendrix MMRM, De With G. PZT-5A4/PA and PZT-5A4/PDMS piezoelectric composite bimorphs. Smart Mater Struct 2014;23:0–8. https://doi.org/10.1088/0964-1726/23/2/025029.

[24] Yun JS, Jeong YH, Nam J, Cho J, Paik J. Development of Stretchable PZT / PDMS Nanocomposite Film with CNT Electrode 2013;22:400–3.

[25] Mamada S, Yaguchi N, Hansaka M, Yamato M, Yoshida H. Performance improvement of piezoelectric-rubber by particle formation of linear aggregates. J Appl Polym Sci 2014;131:1–8. https://doi.org/10.1002/app.39862.

[26] Mamada S, Yaguchi N, Hansaka M, Yamato M, Yoshida H. Matrix influence on the piezoelectric properties of piezoelectric ceramic/polymer composite exhibiting particle alignment. J Appl Polym Sci 2015;132:1–9. https://doi.org/10.1002/app.41817.

[27] Cazacu M, Racles C, Vlad A, Antohe M, Forna N. Silicone-based Composite for Relining of Removable Dental Prosthesis. J Compos Mater 2009;43:2045–55. https://doi.org/10.1177/0021998309340447.

[28] Quinsaat JEQ, Burda I, Krämer R, Häfliger D, Nüesch FA, Dascalu M, et al. Conductive silicone elastomers electrodes processable by screen printing. Sci Rep 2019;9:1–11. https://doi.org/10.1038/s41598-019-49939-8.

[29] Gun'ko V, Vedamuthu M, Henderson G, Blitz J. Mechanism and Kinetics of Hexamethyldisilazane Reaction with a Fumed Silica Surface. J Colloid Interface Sci 2000;228:157–70. https://doi.org/10.1006/jcis.2000.6934.

[30] Quinsaat JEQ, Alexandru M, Nüesch FA, Hofmann H, Borgschulte A, Opris DM. Highly stretchable dielectric elastomer composites containing high volume fraction of silver nanoparticles. J Mater Chem A 2015;3:14675–85.

https://doi.org/10.1039/C5TA03122B.

[31] Liu J, Wu S, Zou M, Zheng X, Cai Z. Surface modification of silica and its compounding with polydimethylsiloxane matrix: Interaction of modified silica filler with PDMS. Iran Polym J (English Ed 2012;21:583–9. https://doi.org/10.1007/s13726-012-0062-x.

[32] Nayak S, Kumar Chaki T, Khastgir D. Development of Poly(dimethylsiloxane)/$BaTiO_3$ Nanocomposites as Dielectric Material. Adv Mater Res 2012;622–623:897–900. https://doi.org/10.4028/www.scientific.net/AMR.622-623.897.

[33] Liu H, Cash G, Birtwhistle D, George G. Characterization of a severely degraded silicone elastomer HV insulator-an aid to development of lifetime assessment techniques. IEEE Trans Dielectr Electr Insul 2005;12:478–86. https://doi.org/10.1109/TDEI.2005.1453452.

[34] Xie S-H, Zhu B-K, Wei X-Z, Xu Z-K, Xu Y-Y. Polyimide/BaTiO3 composites with controllable dielectric properties. Compos Part A Appl Sci Manuf 2005;36:1152–7. https://doi.org/10.1016/j.compositesa.2004.12.010.

[35] Rucigaj A, Krajnc M, Sebenik U. Kinetic Study of Thermal Degradation of Polydimethylsiloxane: The Effect of Molecular Weight on Thermal Stability in Inert Atmosphere. Polym Sci 2017;03:6–11. https://doi.org/10.4172/2471-9935.100024.

[36] Fu S-Y, Feng X-Q, Lauke B, Mai Y-W. Effects of particle size, particle/matrix interface adhesion and particle loading on mechanical properties of particulate–polymer composites. Compos Part B Eng 2008;39:933–61. https://doi.org/10.1016/j.compositesb.2008.01.002.

[37] Qi L, Lee BI, Chen S, Samuels WD, Exarhos GJ. High-Dielectric-Constant Silver-Epoxy Composites as Embedded Dielectrics. Adv Mater 2005;17:1777–81. https://doi.org/10.1002/adma.200401816.

[38] Shen Y, Lin Y, Li M, Nan C-W. High Dielectric Performance of Polymer Composite Films Induced by a Percolating Interparticle Barrier Layer. Adv Mater 2007;19:1418–22. https://doi.org/10.1002/adma.200602097.

[39] Molberg M, Leterrier Y, Plummer CJG, Löwe C, Opris DM, Clemens F, et al. Elastomer actuators: systematic improvement in properties by use of composite materials. Electroact Polym Actuators Devices 2010 2010;7642:76420M. https://doi.org/10.1117/12.847493.

[40] Calebrese C, Hui L, Schadler L, Nelson J. A review on the importance of

nanocomposite processing to enhance electrical insulation. IEEE Trans Dielectr Electr Insul 2011;18:938–45. https://doi.org/10.1109/TDEI.2011.5976079.

[41] Chen Y, Guan J-G, Xie H-Q. An efficient way to prepare silver nanorods in high concentration by polyol method without adding other metal or salt. Mater Chem Phys 2012;134:686–94. https://doi.org/10.1016/j.matchemphys.2012.03.051.

[42] Chen RS, Ahmad S, Ghani MHA, Salleh MN. Optimization of high filler loading on tensile properties of recycled HDPE/PET blends filled with rice husk. AIP Conf Proc 2014;1614:46–51. https://doi.org/10.1063/1.4895168.

[43] Kourki H, Mortezaei M, Navid Famili MH. Prediction of the viscoelastic response of filler network in highly nanofilled polymer composites. J Compos Mater 2015;49:3799–807. https://doi.org/10.1177/0021998314568800.

[44] Amer I, Reenen A Van, Mokrani T. Molecular weight and tacticity effect on morphological and mechanical properties of Ziegler – Natta catalyzed isotactic polypropylenes. Polímeros 2015;25:556–63.

[45] Deutz DB, Mascarenhas NT, van der Zwaag S, Groen WA. Poling piezoelectric (K,Na,Li)NbO_3 -polydimethylsiloxane composites. Ferroelectrics 2017;515:68–74. https://doi.org/10.1080/00150193.2017.1360110.

[46] Chaipanich A. Effect of PZT particle size on dielectric and piezoelectric properties of PZT-cement composites. Curr Appl Phys 2007;7:574–7. https://doi.org/10.1016/j.cap.2006.11.036.

[47] Tao H, Wu J. New poling method for piezoelectric ceramics. J Mater Chem C 2017;5:1601–6. https://doi.org/10.1039/C6TC05328A.

[48] Han P, Pang S, Fan J, Shen X, Pan T. Highly enhanced piezoelectric properties of PLZT/PVDF composite by tailoring the ceramic Curie temperature, particle size and volume fraction. Sensors Actuators A Phys 2013;204:74–8. https://doi.org/https://doi.org/10.1016/j.sna.2013.10.011.

[49] Lee HG, Kim HG. Influence of Microstructure on the Dielectric and Piezoelectric Properties of Lead Zirconate-Polymer Composites. J Am Ceram Soc 1989;72:938–42. https://doi.org/doi:10.1111/j.1151-2916.1989.tb06248.x.

[50] Bhavanasi V, Kumar V, Parida K, Wang J, Lee PS. Enhanced Piezoelectric Energy Harvesting Performance of Flexible PVDF-TrFE Bilayer Films with Graphene Oxide ACS Appl Mater Interfaces 2016;8:521–9. https://doi.org/10.1021/acsami.5b09502.

[51] Ma SW, Fan YJ, Li HY, Su L, Wang ZL. Flexible Porous Polydimethylsiloxane / Lead Zirconate Titanate- Based Nanogenerator Enabled by the Dual Effect of Ferroelectricity and Piezoelectricity. ACS Appl Mater Interfaces 2018;10:33105–11. https://doi.org/10.1021/acsami.8b06696.

Declaration of interests

☒ The authors declare that they have no known competing financial interests or personal relationships that could have appeared to influence the work reported in this paper.

☐The authors declare the following financial interests/personal relationships which may be considered as potential competing interests: